Research Signpost
37/661 (2), Fort P.O.
Trivandrum-695 023
Kerala, India

Computational Methods in Nonlinear Acoustics: Current Trends, 2011: 21-31
ISBN: 978-81-308-0445-3 Editors: Christian Vanhille and Cleofé Campos-Pozuelo

2. Numerical methods for nonlinear acoustic resonators

Xiaofan Li[1] and Ganesh Raman[2]
[1]*Department of Applied Mathematics, Illinois Institute of Technology, Chicago, IL60616, USA*
[2]*Department of Mechanical, Materials and Aerospace Engineering, Illinois Institute of Technology Chicago, IL60616, USA*

Abstract. For the study of pressure waves in an oscillating acoustic resonator, one has to solve the compressible Navier-Stokes equations. The geometry of the resonator strongly influences its resonance frequencies and the nonlinear standing pressure waveform generated within the cavity. Studying the acoustic wave by real physical experiments would be expensive due to the cost of constructing different resonator configurations. Hence, one relies on numerical simulations to study the pressure wave in oscillating resonators. Numerical studies become more challenging due to a possible need for a high-frequency driving force. In this chapter, we review the numerical methods used to simulate the evolution of the pressure wave in oscillating resonators. We also present a numerical method for optimizing resonator shapes in order to maximize the pressure compression ratio, defined as the ratio of maximum to minimum gas pressure at one end of the oscillating resonator.

Correspondence/Reprint request: Dr. Xiaofan Li, Department of Applied Mathematics, Illinois Institute of Technology, Chicago, IL60616, USA. E-mail: lix@iit.edu

I. Introduction

The shape of an oscillating closed cavity is a critical factor in determining the waveform of the standing wave in the resonator. If the shape is a straight cylinder, then shocks forms when the interior gas oscillates at its resonance frequency. High-amplitude and shock-free acoustic pressures can be obtained by varying the shape of resonators. This was first exploited by Lawrenson *et al.*[1] and is referred to as Resonant Macrosonic Synthesis (RMS). Their studies reported that an axisymmetric tube of the shape of a hone-cone can achieve peak acoustic pressures that are three to four times larger than the ambient pressure and the ratio of maximum to minimum pressure can reach 27. The search for the optimal shape is accomplished by mathematical modeling and numerical simulation of RMS, which is shown in a companion paper by Ilinskii *et al.*[2]. The model is improved in Ilinskii *et al.*[3] by accounting for the energy losses in the boundary layer along tube wall. The relation between the natural frequency of a nonlinear acoustic resonator and its shape and the interactions among the modes in the resonator was investigated analytically in Hamilton *et al.*[4].

Studying the acoustic wave by real physical experiments would be expensive due to the cost of constructing different resonator configurations. Hence, we rely on numerical simulations to study the pressure wave in oscillating resonators. This paper provides a review of the numerical methods used in these studies. In Sec. II, we present the modeling equations that describe the motion of gas or fluid in a moving cavity; in Sec. III, we discuss different numerical schemes for solving the model equations; in Sec. IV, we describe the numerical methods for optimizing the shapes.

II. Governing equations

The governing equations for the acoustic field in an oscillating resonator driven by an external force $\boldsymbol{f} = (f_1, f_2, f_3)$ are Navier-Stokes equations for a compressible fluid.[5] The density of the gas ρ, the velocity $\boldsymbol{u}=(u_1, u_2, u_3)$ satisfy the conservation of mass

$$\frac{\partial \rho}{\partial t} + \frac{\partial (\rho u_i)}{\partial x_i} = 0, \tag{1}$$

and the conservation of momentum

$$\frac{\partial (\rho u_i)}{\partial t} + \frac{\partial (\rho u_i u_k)}{\partial x_k} = -\frac{\partial \rho}{\partial x_i} + \frac{\partial \sigma_{ik}}{\partial x_k} + f_i \tag{2}$$

where p is the pressure, $\sigma_{ik} = \eta\left(\frac{\partial u_i}{\partial x_k} + \frac{\partial u_k}{\partial x_i} - \frac{2}{3_i}\delta_{ik}\frac{\partial u_l}{\partial x_l}\right) + \zeta\,\delta_{ik}\frac{\partial u_l}{\partial x_l}$ is the viscous stress and δ_{ik} is the Kronecker delta tensor. Shear viscosity is denoted as η, and ζ is the bulk viscosity that results from nonequilibrium deviations between the actual local pressure and the thermodynamic pressure. Furthermore, the energy density $e = \frac{1}{2}\rho u_k^2 + \varepsilon$ satisfies the conservation of energy

$$\frac{\partial e}{\partial t} + \frac{\partial[(e+p)u_k)]}{\partial x_k} = \frac{\partial}{\partial x_k}(\kappa\frac{\partial T}{\partial x_k}) + \frac{\partial(u_i\sigma_{ik})}{\partial x_k} + f_k u_k, \tag{3}$$

where ε is the internal energy that satisfies the equation of state for an ideal gas $\varepsilon = c_v\rho T = \frac{p}{\gamma - 1}$. T is the temperature, κ is the thermal conductivity, and $\gamma = c_p/c_v$ is the ratio of the specific heats c_p and c_v at constant pressure and volume, respectively. Note that the conservation equations are given in the coordinate frame that is fixed with respect to the resonator.

III. Numerical methods

In this section we review numerical methods for solving the governing equations (1)—(3) or their simplified versions that have been applied to study the wave forms in a closed, oscillating resonator. We discuss these methods in the order of their publication dates.

A. Spectral method

The work by Ilinksii *et al.*[2,3] includes the derivation for a simplified, one-dimensional model from the complete model Eq. (1)—(3) for computing the acoustic wave field in an axisymmetric resonator. Let's denote the inner radius of the resonator by $r=r(x)$, $0<x<l$, where x is the coordinate along the axis of symmetry. The governing equations become

$$\frac{\partial \rho}{\partial t} + \frac{1}{r^2}\frac{\partial}{\partial x}\left(r^2\rho u\right) = 0, \tag{4}$$

$$\frac{\partial u}{\partial t} + u\frac{\partial u}{\partial x} = -\frac{1}{\rho}\frac{\partial p}{\partial x} - a(t) + \frac{(\zeta + 4\eta/3)}{\rho}\frac{\partial}{\partial x}\left(\frac{1}{r^2}\frac{\partial}{\partial x}\left(r^2 u\right)\right), \tag{5}$$

where $a(t)$ is the acceleration of the resonator enforced by the external force f and u denotes u_1 in the original model. The state equation is specified by that of an ideal gas $p = p_0(\rho\ /\rho_0)^\gamma$, where p_0 and ρ_0 are the ambient pressure and density respectively. The possible effects of the boundary layer along the

resonator wall and the acoustically generated turbulence on the acoustical field are neglected in this model but were included in a later work by Ilinksii *et al.*[3]. The quasi-one-dimensional compressible Navier-Stokes equations (4) and (5) are solved using a spectral method, where the unknown variables are expressed in terms of finite Fourier series in time. The Fourier coefficients are determined using a shooting method. Both the experimental and numerical results show that the time harmonics of the dependent variables, such as the pressure *p*, decay rapidly as the frequency increases. This ensures that the number of time harmonics, *N*, needed for accurate results is small.

The method expresses the variables in Fourier series and the Eqs. (4) and (5) can be reduced to a system of Ordinary Differential Equations (ODEs) for the Fourier coefficients of the velocity potential φ, defined as $u = \nabla\varphi$:

$$\begin{cases} \dfrac{d\hat{\varphi}_k}{dx} = \dfrac{\hat{v}_k}{r^2}, & for\ k = 1, 2, \cdots, N, \\ \displaystyle\sum_l D_{kl} \frac{d\hat{v}_l}{dx} = f_k, \end{cases} \tag{6}$$

where $v = r^2 \dfrac{\partial\varphi}{\partial x}$, and $\hat{\varphi}_k$, $\hat{v}_k$ and $\hat{a}_k$ are the Fourier coefficients defined as $\varphi = \sum_{k=-N}^{N} \hat{\varphi}_k e^{ik\omega t}$, $v = \sum_{k=-N}^{N} \hat{v}_k e^{ik\omega t}$, $a = \sum_{k=-N}^{N} \hat{a}_k e^{ik\omega t}$. ω is the frequency of the periodic force exerted on the resonator by the shaker. The detailed expressions for $D_{kl} = D_{kl}(\hat{v}_k, \hat{\varphi}_k, x)$ and $f_k = f_k(\hat{v}_k, \hat{\varphi}_k, x)$ are provided in [2]. The no-penetration boundary conditions at the two ends require that the velocity vanish at $x = 0$ and *l*. Each of the ODEs in Eq. (6) is solved by a shooting or multiple shooting methods using a fifth-order Runge-Kutta scheme with adaptive step-size control.

B. Finite difference methods

1D models

Vanhille and Campos-Pozuelo [6,7] considered a similar one-dimensional nonlinear wave equation

$$\rho_0 \nu b \frac{\partial^3 v}{\partial t \partial x^2} + \rho_0 \frac{\partial^2 v}{\partial t^2} = \frac{\chi(p_0 + \Pi)}{(1 + \frac{\partial v}{\partial x})^{\chi+1}} \frac{\partial^2 v}{\partial x^2}, \tag{7}$$

where *v* is the displacement, ν is the kinematic shear viscosity, Π and χ are the characteristic constants of the fluid in the resonator, and *b* is the viscosity

number. The isentropic state equation of Tait-Kirkwood is used, $(p+\Pi)/(p_0+\Pi)=(\rho/\rho_0)^{\chi}$. The authors solved Eq.(7) by a finite difference method. In particular, the derivatives appearing the equation are approximated by central differencing schemes. The resulting discretized equation is given by

$$\rho_0 vb\frac{(V_{j+1}^{n+1}-2V_j^{n+1}+V_{j-1}^{n+1})-(V_{j+1}^{n-1}-2V_j^{n-1}+V_{j-1}^{n-1})}{\Delta t(\Delta x)^2}+\rho_0\frac{(V_j^{n-1}-2V_j^{n}+V_j^{n+1})}{(\Delta t)^2}$$
$$=\frac{\chi(p_0+\Pi)}{(1+\frac{V_{j+1}^n-V_{j-1}^n}{2\Delta x})^{x+1}}\frac{V_{j+1}^n-2V_j^n+V_{j-1}^n}{(\Delta x)^2}, \quad (8)$$

where x_j 's are equally spaced grid points on the x-axis x_{j+1}- $x_j = \Delta x$, t_{n+1}-t_n=Δt is time step size, and V_j^n denotes the numerical solution of v at the mesh point (x_j, t_n). The finite difference scheme (8) is a 3-time-level implicit method with truncation error $O((\Delta x)^2+(\Delta t)^2)$. The authors investigated the consistency, stability and convergence of the linearized scheme corresponding to Eq.(6). The results were used to monitor the nonlinear calculation by taking a local linearization of the equation.

Independently, Chun and Kim [8] considered an axi-symmetric one-dimensional model that consists of the conservation of mass Eq. (4) and momentum Eq. (5), together with the conservation of energy

$$\frac{\partial p}{\partial t}+\gamma p\frac{\partial u}{\partial x}+u\frac{\partial p}{\partial x}=-\gamma p u\frac{1}{S}\frac{dS}{dx}, \quad (9)$$

where S is the cross section area of the tube. The authors derived the boundary conditions based on the characteristics of the equations. The fourth-order compact finite difference scheme is used for spatial derives and a fourth-order Adams method is applied for time integration.

2D models

Hamilton *et al.* [9] considered a two-dimensional model based on Eqs.(1-3) for thermoacoustic engines. The reduction of the dimension is due to the assumption that the motion is independent in the direction that is perpendicular to the axis of the resonator and parallel to the plates in the stack. The authors have further reduced the two-dimensional model by ordering spatial derivatives in terms of rapid variations across the pores in the stack, versus slow variations along the resonator axis. Let's denote x_1 the direction of the resonator axis and x_2 the direction normal to both the

plates and the resonator. The most significant part of the reduced model that is related to numerical stability is that the x_2 –component of the momentum equation dropped out of the equation, which allows the time-step size to be larger by several orders of magnitude. This is due to the fact that the thickness of the plates is much smaller than that of the distance between two neighboring plates, which is much smaller than the length of the resonator.

To solve the reduced equations of (1—3), the authors used a splitting method: evolve one time-step Δt by three sub-steps. The splitting method works as follows. Decompose the right-hand-side of the conservation laws into three groups: i) x_1 –derivatives terms only; ii) x_2-derivatives terms except those associated with u_2; iii) the rest of the terms. In the first sub-step, advance the unknowns with the terms in the first group using a two-step Lax-Wendroff scheme. In the second sub-step, a semi-implicit scheme is used. To illustrate this, consider the equation

$$\frac{\partial(\rho u_1)}{\partial t} = \frac{\partial}{\partial x_2}(\eta \frac{\partial u_1}{\partial x_2}), \tag{10}$$

where $\eta = \eta(x_2,t)$. The algorithm for integrating Eq.(10) is given by

$$\frac{\rho_j^n U_j^{n+1} - \rho_j^n U_j^n}{\Delta t} = \frac{(\eta_{j+1}^n + \eta_j^n)U_{j+1}^{n+1} - (\eta_{j+1}^n + 2\eta_j^n + \eta_{j-1}^n)U_j^{n+1} + (\eta_{j-1}^n + \eta_j^n)U_{j-1}^{n+1}}{2(\Delta x)^2}, \tag{11}$$

where η_j^n denotes the numerical solution of η at $(x_2, t) = (x_j, t_n)$ and similarly for other variables. It is called semi-implicit because it is implicit with regard to the variable u_1 and is explicit with regard to ρ and η. In the third sub-step, the algorithm ensures that no transverse pressure gradient be allowed in the first two sub-steps.

Vanhille and Campos-Pozuelo [10,11] also used a finite difference method to solve nonlinear waves in two-dimensional resonators and three-dimensional axisymmetric resonators. They assumed the fluid is irrotational and an ideal gas and reduced the conservation laws into a vectorial wave equation

$$\rho_0 \frac{\partial^2 \boldsymbol{u}}{\partial t^2} = \eta \Delta \frac{\partial \boldsymbol{u}}{\partial t} + \left(\zeta + \frac{\eta}{3}\right) \nabla \left(\nabla \cdot \frac{\partial \boldsymbol{u}}{\partial t}\right) + p_0 \gamma \frac{\nabla(\nabla \cdot \boldsymbol{u})}{(1 + \nabla \cdot \boldsymbol{u})^{\gamma+1}}, \tag{12}$$

along with the irrotational condition $\nabla \times \boldsymbol{u} = \boldsymbol{0}$. The derivatives in Eq. (12) are approximated by central differencing except the nonlinear term that is approximated by forward differencing. The resulting scheme is an implicit method with three-time levels. The overall truncation error of the method is $O(\Delta x + (\Delta t)^2)$.

C. Finite element methods

Erickson and Zinn [12] considered the same one-dimensional model, Eqs. (4) and (5), as in Ilinksii *et al.*[2] but used a Galerkin method for the numerical solutions. Manipulating the mass, momentum, and state equations Eqs. (4) and (5), Ilinksii *et al.*[2] derived the dimensionless nonlinear wave equation for the velocity potential Φ

$$\frac{\partial^2\Phi}{\partial T^2}-\frac{1}{\Omega^2\pi^2}\left[\left(\frac{1}{R}\frac{dR}{dX}\right)\frac{\partial\Phi}{\partial X}+\frac{\partial^2\Phi}{\partial X^2}\right] = -\frac{2}{\Omega}\frac{\partial^2\Phi}{\partial X\partial T}\frac{\partial\Phi}{\partial X}-\frac{\gamma-1}{\Omega}\frac{\partial\Phi}{\partial T}\left[\frac{\partial^2\Phi}{\partial X^2}+\left(\frac{1}{R}\frac{dR}{dX}\right)\frac{\partial\Phi}{\partial X}\right]-\Gamma(X,T)+\Theta(X,T), \quad (13)$$

where X, T and R are the non-dimensional axial distance, time and cross-sectional area of the resonator. $\Gamma(X,T)$ and $\Theta(X,T)$ are the external forcing term and the viscous dissipation respectively. The Galerkin method in [12] expands the unknown velocity potential in terms of the trial functions $\{\Psi_n\}$,

$$\Phi(X,T)=\sum_{n=1}^{N}\theta_n(T)\Psi_n(X). \quad (14)$$

In [10], the trial functions $\{\Psi_n\}$ are chosen to be the eigenfunctions for the linear wave equation corresponding to the left-hand side of Eq. (13). For certain resonator shapes, the eigenfunctions $\{\Psi_n\}$ can be found analytically and form an orthogonal basis with an appropriate weight function $W(X)$. For example, if the resonator is of exponential horn shape, $R(X)=R_0\exp(cX)$, then the eigenfunctions $\{\Psi_n\}$ are an orthogonal set of functions with the weight function $W(X)=R(X)$, given by

$$\Psi_n(X)=\exp\left(-\frac{cX}{2}\right)\left(\cos(n\pi X)+\frac{c}{2n\pi}\sin(n\pi X)\right), n=1,2,3,\ldots \quad (15)$$

The Galerkin method consists of the following steps: 1) substitute the expansion (14) into Eq. (13), 2) integrate with $\Psi_j(X)\,W(X)$, for $j=1,2,\ldots,N$, 3) and solve the resulting system of ODEs

$$\sum_n G_{jn}\ddot{\theta}_n-\sum_n H_{jn}\theta_n+\sum_n\sum_m Z_{jnm}\dot{\theta}_n\theta_m+\sum_n(E_{jn}(T)-L_{jn}(T))=0, \text{ for } j=1,2,\ldots,n, \quad (16)$$

where G_{jn}, H_{jn}, Z_{jnm} are the corresponding integrals associated with the linear processes and the nonlinear coupling respectively. Here, $\ddot{\theta}_n=\frac{d^2\theta}{dT^2}$ and $\dot{\theta}_n=\frac{d\theta}{dT}$. E_{jn} and L_{jn} contain terms associated with the viscous damping and the

forcing respectively. The detailed expressions of these coefficients are given in [12]. We only list two of them as examples,

$$G_{jn} = \int_0^1 W(X)\ \Psi_j(X)\Psi_n(X)dX, \quad H_{jn} = \int_0^1 W(X)\,\Psi_j(X)\left[\frac{d^2\Psi_n}{dX^2} + \left(\frac{1}{R}\frac{dR}{dX}\right)\frac{d\Psi_n}{dX}\right]dX. \quad (17)$$

We note that, if the trial functions $\{\Psi_n\}$ are chosen an orthonormal basis, then most of the terms in the system of ODEs (16) vanish, because $G_{jn}= \delta_{jn}$, where δ_{jn} is the Kronecker delta function, and similar simplification holds for other coefficients.

IV. Methods for shape optimization

Engineering applications constantly involve optimization. Here, we present the method used in [13-15] for optimizing resonator shapes. In this context, one has to solve a system of partial differential equations, Eqs. (4) and (5), to obtain the value of the quantity to be optimized.

The procedures for finding the optimal shape parameters are described as follows. Given an initial resonator shape and a fixed value of maximum external force, the resonance frequency of the resonator is determined and the compression ratio, defined as the maximum-to-minimum pressure ratio at the narrow end of the cavity, is computed. Then, the optimization step is performed yielding the next resonator shape candidate. The first and the second steps are repeated until incremental changes in the resonator contour no longer produce higher compression ratios and the local optimal design is determined.

To simplify the discussion, the following dimensionless variables are introduced,

$$X = \frac{x}{l}, \quad T = \omega t, \quad R = \frac{r}{l}, \quad R_0 = \frac{r_0}{l}, \quad A = \frac{a}{l\omega_0^2}, \quad (18)$$

where ω is the frequency of the periodic force acted on the resonator, $\omega_0 = \pi c_0 / l$ is the fundamental frequency of a cylindrical resonator of length l.

Suppose the resonator shape $R(X)$ is determined by a number of shape parameters, $S_0, S_1, \ldots, S_n$. For example, a cone is given by $R(X) = S_0 + S_1X$. To determine the shape producing the highest value of the pressure compression ratio R_c, i.e.,

$$R_c(S_0, S_1, \cdots, S_n) = \frac{p_{\max}}{p_{\min}}, \text{ at } X=0, \quad (19)$$

gradients of the pressure compression ratio value are compared with the gradients of the shape parameters to indicate the next contour iteration. p_{max} and p_{min} denote the maximum and minimum pressure at the narrow end of the resonator during one period of oscillation respectively. The compression ratio R_c is a function of the shape parameters, the dimensionless frequency Ω, and the history of Ω (due to the existence of hysteresis effects). The method for obtaining R_c for a fixed resonator shape is the spectral method explained earlier in the section. [2,3]

The resonator shape is optimized by holding constant the maximum inertial force required to establish the periodic oscillation. Using Newton's Second Law, for a fixed amount of maximum dimensionless external force F_{max}, the dimensionless acceleration amplitude $\tilde{A}$ is easily deduced from $\tilde{A} = F_{max}/(M + M_a)$, where M is the dimensionless mass of the resonator.

A quasi-Newton method, BFGS (Broyden-Fletcher-Goldfarb-Shanno), then is used for maximizing the multi-variable nonlinear function $R_c(S_0, S_1, \ldots, S_n)$. [16] BFGS is an iterative method, approximating the objective function by a quadratic function at each iteration. At each major iteration step, k, a line search is performed in the direction

$$d^{(k)} = H_k^{-1} \cdot \nabla R_c(S^{(k)}),$$

where $S^{(k)} = (S_0^{(k)}, S_1^{(k)}, \cdots, S_n^{(k)})$ is the vector of the shape parameters at k-th iteration of BFGS. H_k is the BFGS approximation to the Hessian matrix of R_c with respect to S, defined by

$$H_k = H_{k-1} + \frac{q_{k-1} q_{k-1}^T}{q_{k-1}^T q_{k-1}} - \frac{H_{k-1}^T t_{k-1}^T t_{k-1} H_{k-1}}{t_{k-1}^T H_{k-1} t_{k-1}},$$

where $t_{k-1} = S^{(k)} - S^{(k-1)}$, $q_{k-1} = \nabla R_c(S^{(k)}) - \nabla R_c(S^{(k-1)})$ and $H_0 = I$.

The evaluation of the objective function R_c involves solving many iterations of a nonlinear system of ODEs given in Eq. (6), since the gradient information of R_c required for the BFGS method is not available analytically. Using a numerical differentiation method via finite differences, the gradient information is determined by perturbing each design variable, S_i, in turn and calculating the rate of change in the objective function $R_c(S_0, S_1, \ldots, S_n)$.

Figure 1 shows the optimal resonator shapes confined to the three types: conical, hone-cone and cosine shapes. The maximum pressure compression ratio value of 48 is found in an optimized horncone shape.

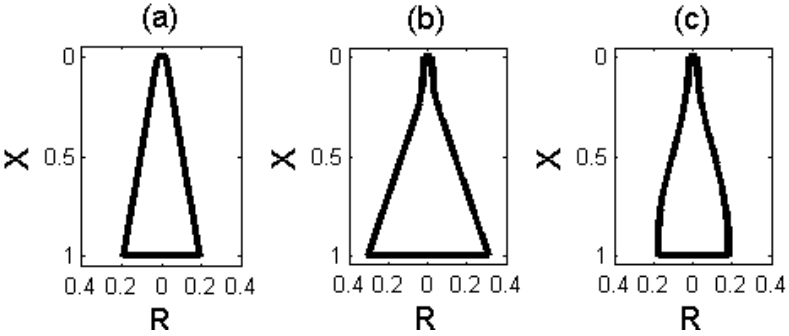

Figure 1. Optimized (a) conical, (b) horncone, and (c) cosine resonator shapes.

References

1. C. C. Lawrenson, B. Lipkens, T. S. Lucas, D. K. Perkins, and T. W. Van Doren, "Measurements of macrosonic standing waves in oscillating closed cavities." J. Acoust. Soc. Am. **104**, 623-636 (1998).
2. Y. A. Ilinskii, B. Lipkens, T. S. Lucas, T. W. Van Doren, and E. A. Zabolotskaya, "Nonlinear standing waves in an acoustical resonator," J. Acoust. Soc. Am. **104**, 2664-2674 (1998).
3. Y. A. Ilinskii, B. Lipkens and E. A. Zabolotskaya, "Energy losses in an acoustical resonator," J. Acoust. Soc. Am. **109**, 1859-1870 (2001).
4. M. F. Hamilton, Y. A. Ilinskii, and E. A. Zabolotskaya, "Linear and nonlinear frequency shifts in acoustical resonators with varying cross sections," J. Acoust. Soc. Am. **110**, 109-119 (2001).
5. L.D. Landau and E.M. Lifshitz, *Fluid Mechanics*, 2nd ed. (Pergamon, New York, 1987)
6. C. Vanhille and C. Campos-Pozuelo, "A high-order finite-difference algorithm for the analysis of standing acoustic waves of finite but moderate amplitude," J. Comput. Phys. **165**, 334-353 (2000).
7. C. Vanhille and C. Campos-Pozuelo, "Numerical model for nonlinear standing waves and weak shocks in thermoviscous fluids," J. Acoust. Soc. Am. **109**, 2660-2667 (2001).
8. Y.-D. Chun and Y.-H. Kim, "Numerical analysis for nonlinear resonant oscillations of gas in axisymmetric closed tubes." J. Acoust. Soc. Am. **108**, 2765-74 (2000).
9. M. F. Hamilton, Y. A. Ilinskii, and E. A. Zabolotskaya, "Nonlinear two-dimensional model for thermoacoustic engines," J. Acoust. Soc. Am. **111**, 2076-2086 (2002).
10. C. Vanhille and C. Campos-Pozuelo, "Numerical simulation of two-dimensional nonlinear standing acoustic waves," J. Acoust. Soc. Am. **116**, 194-200 (2004).

11. C. Vanhille and C. Campos-Pozuelo, "Numerical and experimental analysis of strongly nonlinear standing acoustic waves in axisymmetric cavities," Ultrasonics, **43**, 652-660 (2005).
12. R. R. Erickson and B. T. Zinn, "Modeling of finite amplitude acoustic waves in closed cavities using the Galerkin method," J. Acoust. Soc. Am. **113**, 1863-70 (2003).
13. X. Li, J. Finkbeiner, G. Raman, C. Daniels, and B. Steinetz, "Optimized shapes of oscillating resonators for generating high-amplitude pressure waves", J. Acoust. Soc. Am. **116**, 2814--21 (2004).
14. J. Finkbeiner. *Nonlinear acoustic standing waves in oscillating closed containers*(Master's Thesis, Illinois Institute of Technology, May 2003).
15. X. Li, J. Finkbeiner, G. Raman, C. Daniels, and B. Steinetz, "Nonlinear resonant oscillations of gas in optimized acoustical resonators and the effect of central blockage", AIAA paper No. 2003-0368, *41st AIAA Aerospace Sciences Meeting and Exhibit* 2003 Reno, Nevada.
16. P. E. Gill, W. Murray, and M. H. Wright, *Practical Optimization* (Academic Press, New York, 1981).